JOURNAL OF
MATERIALS PROCESSING
&CHARACTERIZATION

The effect of AA5083H116 2-layer MIG welding speed on physical and mechanical properties

Mudjijana*
V. Malau
U. A. Salim

Department of Mechanical and Industrial Engineering, Faculty of Engineering, Universitas Gadjah Mada. Jl. Grafika 2, Yogyakarta 55281, Indonesia

Email:
*mudjijana@ugm.ac.id

Keywords
AA5083H116, ER5356, 2-layer MIG (metal inert gas), welding speed, physical and mechanical properties.

Abstract
Metal welding can be performed on 1 layer or more depending on the thickness of the plate welded. In the case of 3-mm-thick plates, high-efficiency welding can be carried out on 1 layer if appropriate welding speed, voltage, and amperage are applied. If two layers are to be used, sound weld of 3-mm-thick plates can be achieved if higher welding speed and lower voltage and amperage are applied. This research was intended to conduct 2-layer MIG weld works at welding speeds of ≥10, 13, and 16 mm/s in accordance with previous research studies and to analyze the physical and mechanical properties generated. This research employed the AA5083H116 material, ER5356 electrode, and argon gas. During the welding processes, the thermal cycles were recorded, and after the processes, the welding results were observed for the macro- and microstructures and for the optimal welding speed under an SEM. In addition, tensile tests, Vickers microhardness tests, and corrosion tests were also undertaken. The results show that the 2-layer MIG welding at the welding speed of 10 mm/s produced the best physical and mechanical properties.

Volume 1, Number 1, 2020, 31-40
DOI: http://dx.doi.org/10.22146/jmpc.v1i1.51417
e-ISSN: 2716-1285, ISSN: 2714-9722

1. Introduction

Welding works are commonplace in the construction sector. With the development of manufacturing process, it is important that welds be carried out in maximum efficiencies. Welding technology is continuously developed to achieve better time and production cost effectiveness. In the transportation sector, specifically, welding applications are ubiquitous in shipping, aviation, and rail transport industries. The materials used can range from carbon steels, aluminum alloys, to stainless steels and a range of other materials. It is imperative to welding constructions that attention be given to the compatibility between the types of materials welded, welding electrodes, and welding methods in order to attain sound welds. A 5083 aluminum alloy is a lightweight metal with a low density of 4.5 g/cm3 (Ashby and Jones, 2012). This material is popular owing to its high tensile strength and corrosion resistance. Yazdipour et al. (2011) conducted an inquiry on MIG welding of AA5083 with a variety of parameters, including welding speeds of 7.24–10 mm/s, voltages of 18–22 V, and electrical currents of 120–182 A, and yielded a maximum ultimate tensile strength value of 337 MPa. Kim et al. in their research (2010) obtained from conventional MIG welding of AA5083H116 a tensile strength value of 344.64 MPa in weld metal, which was higher than that in the base metal, with an efficiency of 85.8%. In a separate study, Li et al. (2017) conducted MIG welding with the ER5356 electrode on two dissimilar metals, 7N01-T5 and 7N01-T4, at varied welding speeds of 6.5, 7.5, and 8 mm/x, electrical current of 290 A, and voltage of 27 V. From that research, they obtained weld-zone tensile strength of 283 MPa, which was lower than that in the BM area (360 MPa for 7N01-T5 and 432 MPa for 7N01-T4). From the results of the corrosion test on the 4.0 M NaCl + 0.5 M KNO3 + 0.1 M HNO3 solution medium it was found that 7N01-T4 was more susceptible to corrosion than 7N01-T5. The part most prone to corrosion was the heat affected zone (HAZ), and in general, the weld metal was more susceptible to corrosion than the base metal. Mudjijana et al. (2017) performed characterization of welds of the AA5083H116 material with the ER5356 electrode at varied MIG welding speeds of 8, 10, and 12 mm/s. It was discovered that at the welding speed of 10 mm/s, the highest tensile strength, bending strength, and welding efficiency were achieved. The results of the studies above can be used as a reference for determination of welding speed for 2-layer MIG welding, with an assumption that the heat generated would be higher than that from 1-layer MIG welding. Thus, it was assumed that the 2-layer MIG welding speed should be faster than that applied in 1-layer MIG welds. This research investigated the effect of ER5356-electrode AA5083H116 2-layer MIG welding speeds (in this study 10, 13, 16 mm/s).

2. Materials and Methods

The material used in this research was AA5093H116 300 mm × 75 mm × 3 mm in size, the electrode used was the ER5356 electrode (ASME, 2001) 0.8 mm in diameter, and the shielding gas used was argon. The welding was undertaken on 2 layers with a Tenjima 200S under the scheme provided in Figure 1 with the welding parameters presented in Table 1. During the welding processes, the thermal cycles were measured with type-K thermocouple wire and an NI USB-9162 instrument in the installation position shown in Figure 2. The welding results were subjected to microstructure observations with a 10% NaOH etching solution (AST, 2015), Vickers microhardness tests with a 100 g load, tensile tests per the ASTM-E8 standard, and corrosion tests with potentiodynamic polarization as shown in Figure 3 within a 3.5% NaCl environment with a specimen thickness of ~2 mm and diameter of ~15 mm. The best welding speed was observed under an SEM (scanning electron microscope).

Table 1. Welding parameters

Welding parameters	
Electrode distance from specimen (mm)	10
Welding speed (mm/s)	10, 13, and 16
Welding angle (θ°)	80
Average welding voltage (Volt)	19
Average welding current (Ampere)	110
Filler rate (mm/s)	27
Filler diameter (mm)	0.8
Argon flow (liter/minute)	15
Welding 1-2 pause time (s)	15

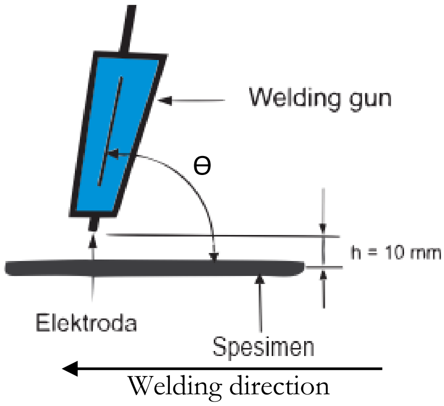

Figure 1. Schematic of welding gun position relative to specimen

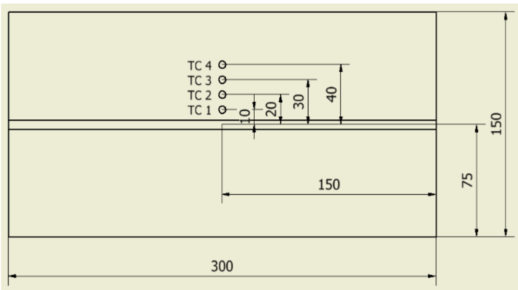

Figure 2. Thermocouple position in specimen

Figure 3. Potentiodynamic polarization corrosion test instrument

3. Results and Discussion

Thermal cycle

Detailed results of the thermal cycle measurement during the welding processes are only provided for the best welding speed of 10 mm/s in Figure 4, while the peak temperatures are presented in Table 2. A sample welding joint generated at the welding speed of 13 mm/s is displayed in Figure 5. The peak TC1 temperatures on layers 1 and 2 at the welding speeds of 10, 13, and 16 mm/s are provided in Table 3. It is shown in the table that the peak temperatures on layer 1 were lower than those on layer 2 because layer 2 had been affected by the initial heating during the welding processes on layer 1 with a pause time of 10 mm/s. The peak temperatures at the welding speed of 10 mm/s were higher than the rest due to bigger heat input based on the equation Q = VI/v, where v is welding speed (mm/s), V is welding voltage (Volt), and I is welding current (Amp).

Table 2. Thermal cycle peak temperatures 10 mm from weld line

Welding speed	Temperature (°C)	
	TC1 peak temperatures on layer 1	TC1 peak temperatures on layer 2
10 mm/s	231.2	244.9
13 mm/s	215.6	241.5
16 mm/s	159.7	183.4

Table 3. Peak temperatures in Figure 4

Specimen	Peak temperatures (°C)			
	TC1	TC2	TC3	TC4
Welding speed of 10 mm/s	231.2	151.1	109.5	97.4
	244.9	172.1	133.5	120

Macro- and micro observation

Macrostructure observation was carried out under a 10× magnitude optical microscope (OM), and the microstructure observation a 200× magnitude optical microscope. The macrostructure observation results in Figure 6 show the differences between the weld zones of base metal (BM), heat affected zone (HAZ), and weld metal (WM). The weld metal was rich in porosity in all specimens. Porosity is a weld defect from the presence of entrapped solved hydrogen during the welding process in the molten metal, where the molten metal freezes before the hydrogen gets to evaporate. It could also be observed that the specimen welded at the speed of 16 m/s experienced incomplete penetration, which is presumed to happen due to a number of factors, namely excessively low welding current, excessively fast welding speed, improper torch angle, and poor welding preparation.

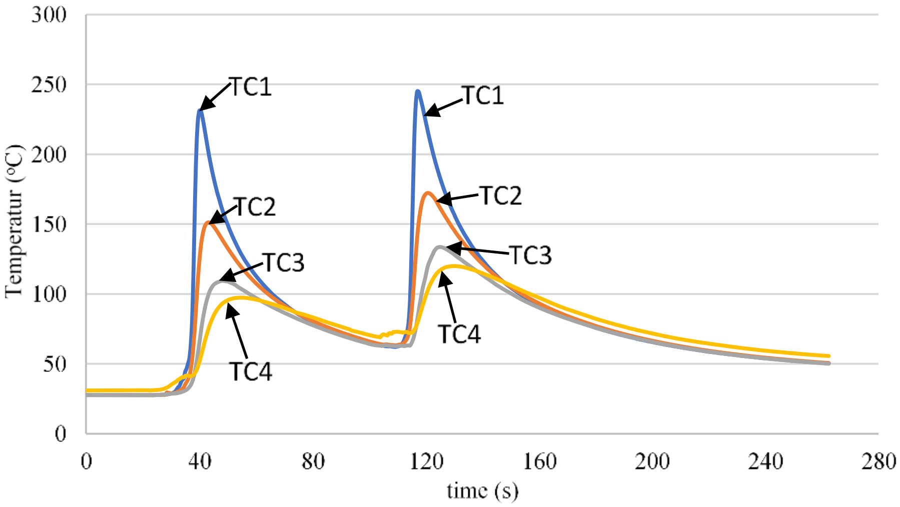

Figure 4. Thermal cycles at welding speed of 10 mm/s

Figure 5. Welding result at welding speed of 13 mm/s

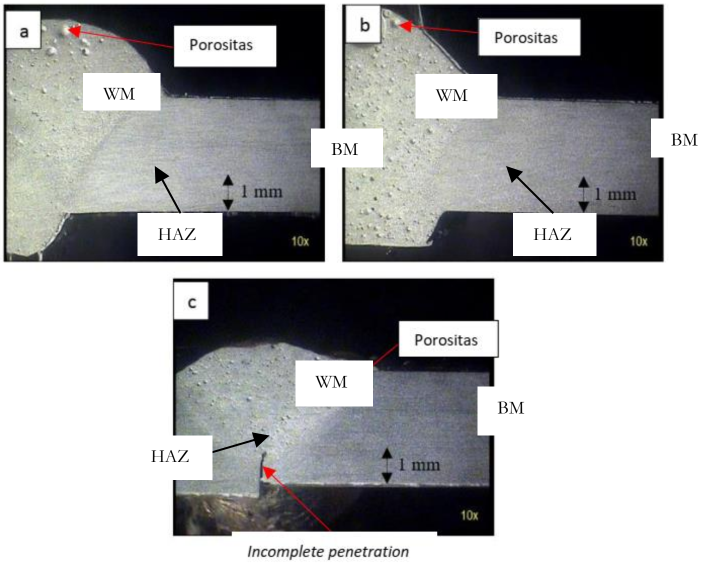

Figure 6. Sectional macrostructure at welding speeds: (a) 10 mm/s, (b) 13 mm/s, and (c) 16 mm/s

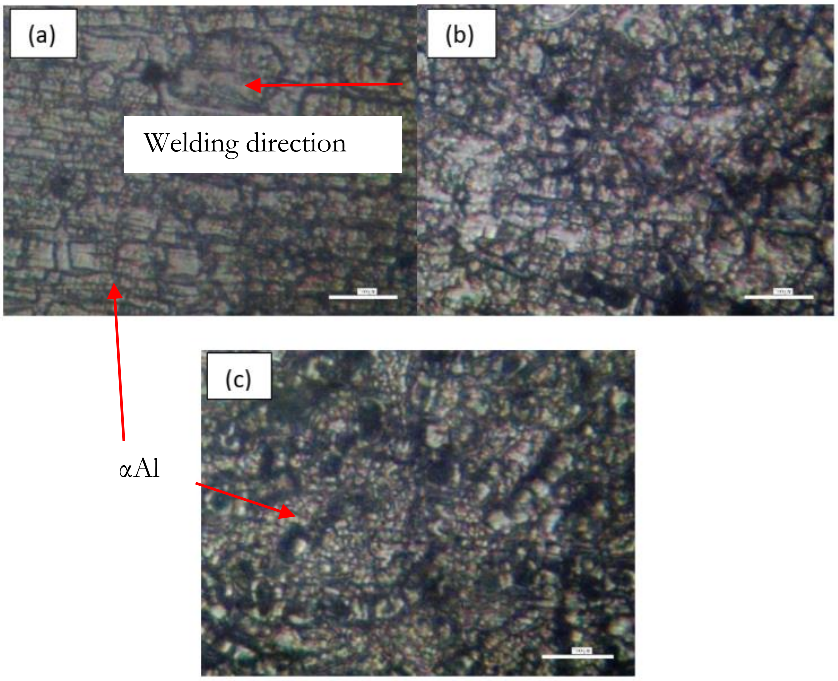

Figure 7. Macrostructure in (a) base metal (BM), (b) heat affected zone (HAZ), and (c) weld metal (WM) at welding speed of 10 mm/s.

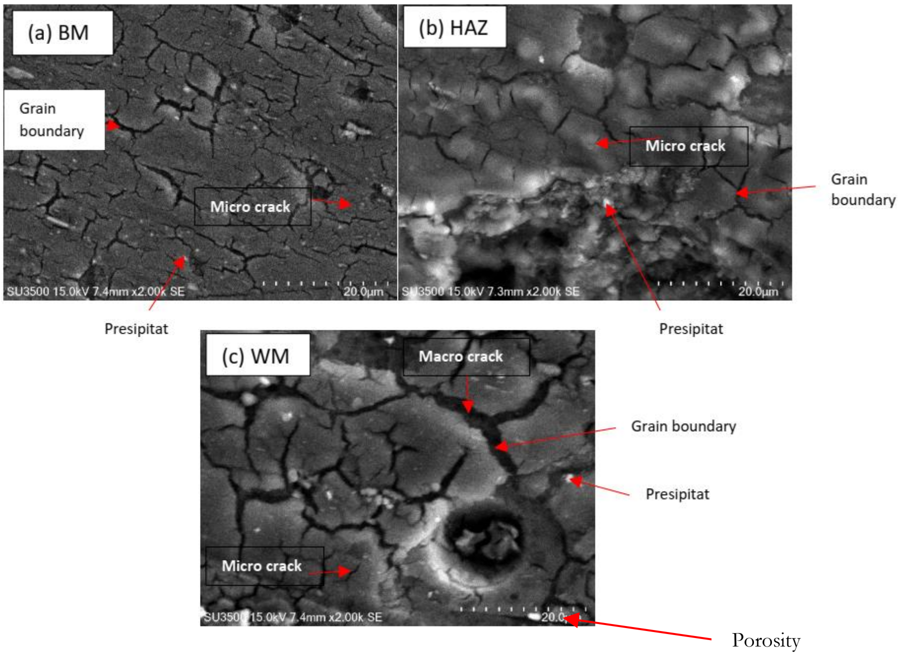

Figure 8. Microstructure under scanning electron microscope (SEM): (a) BM, (b) HAZ, and (c) WM

Microstructure imaging was performed in three different regions, namely base metal (BM), heat affected zone (HAZ), and weld metal (WM), and only the images for the welding speed of 10 mm/s are displayed because the microstructures at the other welding speeds were similar with distinction only in the grain size. The grain size at the welding speed of 10 mm/s was bigger than those at the welding speeds of 13 and 16 mm/s owing to larger heat input. The results of the microstructure observation at the welding speed of 10 mm/s are shown in Figure 7. As exhibited in Figure 7(a), the microstructure in the BM had elongated grains from fabrication with H116 treatment. The BM microstructure was unaffected by the heat produced by the welding process. The HAZ microstructure shown in Figure 7(b) had grains partially similar to those in the BM and partially equiaxed due to WM-BM fusion. Meanwhile, the microstructure in the WM region was almost entirely equiaxed. The αAl appeared white in color for an Al-Mg alloy with an Mg content for AA5083H116 of roughly 4.5%.

The results of the SEM microstructure observation at the welding speed of 10 mm/s are shown in Figure 8 ((a) BM, (b) HAZ, (c) WM). From the SEM results, it can be observed that the grains in the BM were smaller in size than those in the HAZ and WM due to H116 treatment. In the HAZ, the granular sizes were slightly bigger than those in the BM, yet slightly smaller than those in the WM, from heat influence over the welding process. On the other hand, the WM had grains in the largest sizes and in equiaxed shapes; the WM was the ER5356 welding material with air cooling-freezing rate. Microcracks and precipitates were spotted in all the BM, HAZ, and WM. Microcracks in the BM emerged because the H116 treatment performed involved solid solution treatment and rolling up to ¾ hardness. The microcracks in the HAZ were caused by uneven cooling process and non-uniform fusion zone unlike the BM. Meanwhile, the microcracks in the WM were brought about by both small and big grain sizes which caused imbalance in the cooling rate. It is noticeable at the granular boundary that more macrocracking took place than microcracking.

Vickers hardness

Based on Figure 9, Table 3, and Figure 10, the hardness values in the BM from the testing were virtually uniform across the three specimens. The specimen for the welding speed of 10 mm/s yielded an average hardness value of 94.07 VHN, 13 mm/s 93.10 VHN, and 16 mm/s 93.79 VHN. The average hardness value in the HAZ was the highest in the 16 mm/s welding speed specimen, namely 92.21 VHN. In the 13 mm/s welding speed specimen the average value was 83.11 VHN, while 10 mm/s 77.34 VHN. The WM did not exhibit any significant difference in the hardness value between welding speeds. The specimen for the welding speed of 16 mm/s had the highest average hardness value of 72.96 VHN, followed by those for the welding speeds of 13 mm/s and 10 mm/s with 70.94 VHN and 69.84 VHN, respectively.

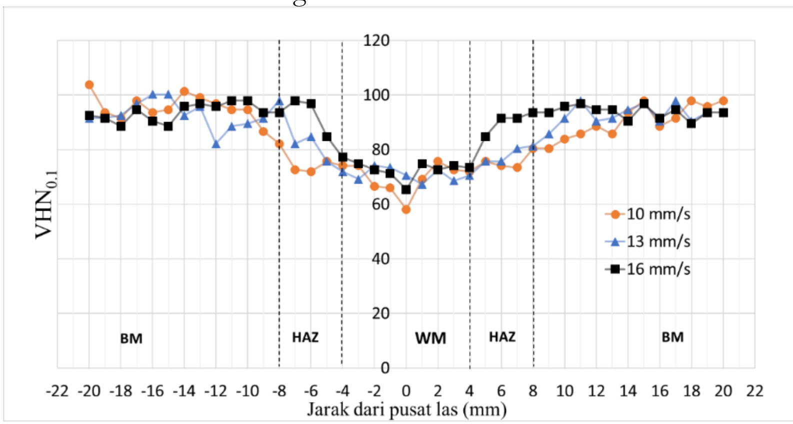

Figure 9. Hardness value comparison

Table 4. Average hardness values

Welding speed	BM	HAZ	WM
	Average Vickers hardness value		
10 mm/s	94.07	77.34	69.84
13 mm/s	93.10	83.11	70.94
16 mm/s	93.79	92.21	72.96

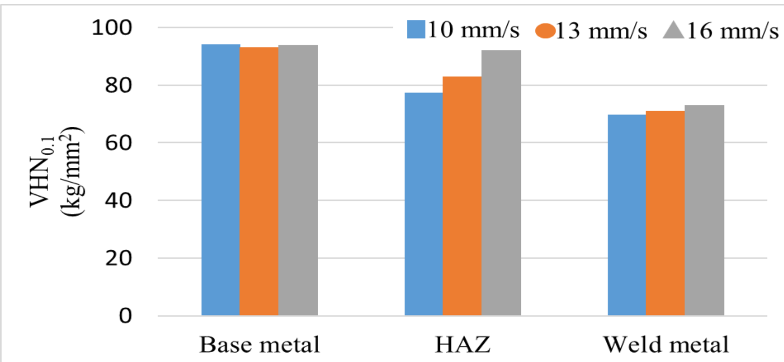

Figure 10. Comparison of average hardness values in BM, HAZ, and WM

In Figure 10 it can be observed that the Vickers hardness value-distance to weld core curve for every weld variation had a similar trend line to another variation. The lowest hardness values were found in the WM, which increased in the HAZ and achieved maximums in the BM. The HAZ exhibited lower hardness values than the BM. Series 5xxx aluminum alloys are non-heat treatable, thus the strength cannot be increased by applying heat. The decrease in hardness value in the HAZ can be associated with microstructure. The HAZ had bigger grains than the BM, causing the strength to withstand dislocation to go down. The lowest hardness value in the WM, too, is tied to microstructure. Compared to the BM and HAZ, the WM had larger granular sizes giving it the lowest strength to withstand dislocation. The 16 mm/s welding speed specimen, which received the smallest heat input, yielded the highest hardness value, while the 10 mm/s welding speed specimen, which received the most heat input, did the lowest hardness value. Series 5xxx aluminum alloys can be subjected to work hardening, which can cause alteration to the microstructure. A rolling or work hardening process is a key factor that gives the BM greater hardness than the WM (Yazdipour dkk, 2011).

Tensile Test

The results of the tensile test per the ASTM-E8 are provided in Figure 11. The yield strength value of 292.52 MPa and tensile strength value of 360.31 MPa of the raw material were to be compared with the yield and tensile strength of the 2-layer MIG weld specimens. At the welding speed of 10 mm/s, the specimen had the greatest yield strength and tensile strength (230,95 Mpa and 281.07 MPa, respectively), thus the maximum welding efficiency (welding efficiency = the tensile strength of the welded material divided by the tensile strength of the raw material = 78%). The specimens at the welding speeds of 13 mm/s and 16 mm/s had lower yield strength and tensile strength (Figure 11). The 2-layer MIG welding efficiency was indistinct from that of 1-layer MIG welding as studied by Mudjijana et al. (2017). Hence, the plate thickness of 3 mm is not suited for 2-layer welding.

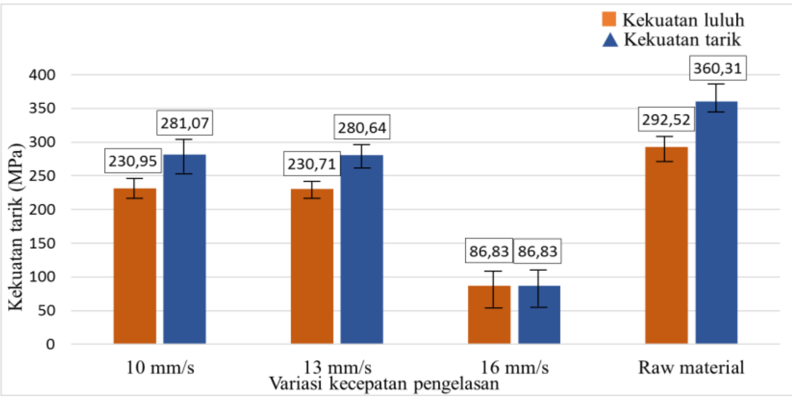

Figure 11. Tensile strength vs welding speed variation

Potentiodynamic polarization corrosion test

The results of the corrosion test with the potentiodynamic polarization method (potential (V) vs current density comparison (A/cm^2)) are presented in Figure 12. Through calculations, corrosion rates were obtained and are presented in Table 4. BM had the lowest corrosion rate, namely 0.253 mm/year. The specimen for the welding speed of 10 mm/s produced a corrosion rate of 0.285 mm/year, 13 mm/s 0.277 mm/year, and 16 mm/s 0.450 mm/year.

The corrosion rate in the weld zone was higher than the base material, in which case, the corrosion rate in the weld zone would increase with welding speed. Al-Mg alloys have good resistance to corrosion (Wiryosumarto, 2000). Variation in heat input amount leads to variation in precipitate amount in WM, while variation in precipitate variation leads to variation in Ecorr and Icorr values in WM. The more precipitate amount in WM, the higher the Ecorr and Icorr values and the faster the corrosion rate. A defect in WM in the form of porosity also plays a role in the acceleration of the corrosion rate. Corrosion will attack the weakest region in which defects are found. Varying corrosion resistance rates across weld joint locations are dependent on the distribution, sizes, and types of precipitates and the chemical composition (Li et al., 2017).

Table 5. Corrosion rates of BM and 2-layer MIG welding result

Material	Welding speed (mm/s)	E_{corr} (mV)	I_{corr} (μA)	Corrosion rate (mm/ year)
Base material	-	-743.14	22.34	0.25
Weld zone	10	-733.91	25.12	0.29
	13	-751.42	33.23	0.38
	16	-759.60	39.70	0.45

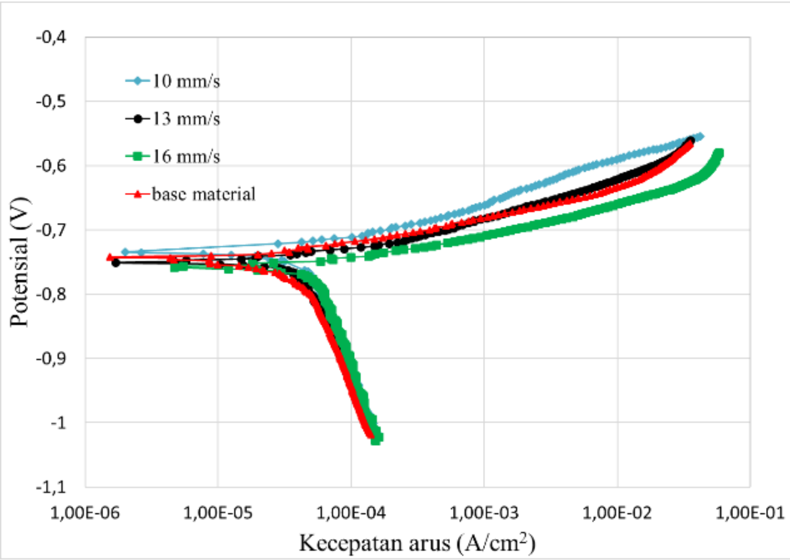

Figure 12. Potential (V) vs current density (A/cm²)

4. Conclusion

Based on the testing on the 2-layer MIG welding joints obtained at different welding speeds (10, 13, 16 mm/s), it can be concluded that (1) an increase in the welding speed causes a decrease in the maximum temperature achieved, leading to lowered heat input received by the specimen and lowered tensile strength; (2) an increase in the welding speed causes an increase in the hardness in the HZ and BM; and (3) an increase in the welding speed causes a decrease in the resistance to corrosion in the weld zone, in which case, the BM has better corrosion resistance than the WM.

5. Acknowledgements

Gratitude is due to the Minister of Research, Technology, and Higher Education, who have funded this research under the UGM PDD contract no. 1769/UN1/DITLIT/DIT-LIT/LT/2018, the Department of Mechanical and Industrial Engineering of the Faculty of Engineering, UGM, for the opportunity, and Mr. Ekak, Mr. Sunhaji, Mr. Yasin, and Mr. Arief, for assisting with this research.

6. References

Ashby, M. F. dan Jones, D. R. H., 2013, Engineering Materials 2: An Introduction Microstructures and Processing, 4thed, Butter-worth-Heinemann, p. 190.

ASME, 2001, Materials Part C – Specifications for Welding Rods, Electrodes, and Filler Metals, ASME, New York.

ASTM, 2009, E8/E8M-09, Standard Test Method for Tension Testing of Metallic Materials, ASTM International.

ASTM, 2015. E407-07 (Reapproved 2015), Standard Practice for Micro-etching Metals and Alloys, ASTM International.

Haelsig, A., Kusch, M., Mayr, P., 2012, New Findings on The Efficiency of Gas Shielded Arc Welding. 56, pp. 98-104.

Kim, S-J., Kim, S-K., Park, J-C., 2010, The Corrosion and Mechanical Properties of Al Alloy 5083-H116 in Metal Inert Gas Welding Based on Slow Strain Rate Test. Surface & Coatings Technology, 205, pp. S73–S78.

Li, S., Dong, H, Shi, L., Li, P., Fe., Y. 2017, Corrosion Behavior and Mechanical Propertieso of Al-Zn-Mg Aluminum Alloy Weld, Corrosion Science, 123, pp. 243–255.

Mudjijana, Ilman, M.N., Iswanto, P.T., 2017, Karakterisasi Pengaruh Kecepatan Las pada Pengelasan MIG AA 5083 H116 dengan Elektroda ER 5356, POROS, Volume 15 Nomor 1, pp. 26-34.

Wiryosumarto, H., 2000, Teknologi Pengelasan Logam, PT Pradnya Paramita, Jakarta.

Yazdipour, A.R., Shafiei, L., Aval, H.J., 2011, An Investigation of The Microstructures and Properties of Metal Inert Gas and Friction Stir Welds in Aluminum Alloy 5083, Sadhana, Vol. 36, pp.50